Preprints of the 21st IFAC World Congress (Virtual)
Berlin, Germany, July 12-17, 2020

Performance-based Fault Mitigation in Sampled-Data Process Systems with Sensor Faults and Measurement Delays

James Allen, Nael H. El-Farra *

* *Department of Chemical Engineering, University of California, Davis, CA 95616* (e-mail: nhelfarra@ucdavis.edu)

Abstract: The objective of this work is to provide systematic tools for the analysis and mitigation of sensor faults in sampled-data processes with discretely-sampled and delayed state measurements. The emphasis is on determining the effects of varying process and controller parameters, including faults, sampling period, delay, plant-model mismatch and controller gain, on the stability and performance characteristics of the closed-loop system, and providing insight into how these effects can be counteracted through the use of active fault accommodation measures. The developed insights and methods are applied to a representative chemical process system with sampled and delayed state measurements. The stability of the closed-loop system is first characterized as a function of the sampling rate, the measurement delay, the fault magnitude, the fault accommodation measures, and the plant-model mismatch. The faults assessed have the form of diminished or hyperactive measurements of the system states. As a primary accommodation measure for these faults, the location of the closed-loop poles are adjusted to achieve stability during faulty operation. A performance metric that captures the closed-loop system's disturbance recovery behavior is chosen and parameterized in the same manner as the stability of the system, and is used to inform the fault accommodation decision-making process further. The explicit characterization of the stability and performance regions offer insight into the operational robustness and ranges of tolerable sensor faults that can be accommodated; and these are discussed with some simulation results for context.

Keywords: Sensor faults, fault accommodation, sampled-data systems, measurement delay, chemical processes.

1. INTRODUCTION

The ability to operate a process safely and profitably despite faulty conditions in the process or control system components is an increasingly critical requirement of modern-day process systems. The fundamental and practical significance of this problem have motivated significant research work leading to an extensive body of work on the analysis, design and implementation of fault-tolerant control systems (see, for example, Blanke et al. (2003); Isermann (2005); Mhaskar et al. (2013)). This problem has classically been studied in the context of conventional feedback control systems which assume that continuous state and/or output measurements are available from the sensor to the controller. Due to advances and cost reduction in sensing technologies, discrete sampled-data measurements are becoming more common in industrial processes. This has implications for the control scheme for such systems as continuous measurement of system data often proves logistically or technologically prohibitive with these sampled-data sensors. In such systems, the stability and performance of the closed-loop system (and hence its fault-tolerance capabilities) are directly linked to the sampled measurement frequency. This has motivated a series of prior works addressing the problem of fault-tolerant control in the context of sampled-data process systems using active control structure reconfiguration (Sun and El-Farra (2011)) and stability-based fault accommodation approaches (Napasindayao and El-Farra (2013)). These works were extended in Napasindayao and El-Farra (2015) to include an optimization-based approach for fault estimation to aid in the fault accommodation framework and in Allen and El-Farra (2017) to incorporate performance considerations in the fault accommodation logic in the context of faulty control actuators.

The majority of these prior works maintained a focus on control actuator faults, with relatively little attention dedicated to handling sensor faults. However, sensor faults are common and often critical to the performance of the overall system. This is especially evident in the case of dense sensor deployment and large sensor networks, which are common in many industrial applications. Examples of previous works on this subject include studies on passive fault-tolerant control approaches in the context of sensor data losses (e.g., Gani et al. (2008)), sensor reconfiguration-based approaches (e.g., Yao and El-Farra (2014)), stability-based accommodation using delayed measurements (e.g., Peng and El-Farra (2015)), and performance-based accommodation of systems with multi-rate sensor faults (e.g., Allen et al. (2019)).

While this growing body of work has looked separately into the issues of stability, performance, delays and sensor

faults, as a whole there has not been any rigorous assessment or examination of the implications and nuances that occur when these factors are addressed at once. In particular, the model's time evolution exhibits multiple discrete instances of discontinuity as a consequence of the update schemes required in sampled-data models, as discussed in the case of actuator faults in Allen et al. (2019). Because of these discontinuities, the effects of measurement delays on the performance characterization of such systems are especially complex, and to date those effects have not been explored in the context of sampled-data systems with sensor faults. This study aims, in part, to address this gap.

Motivated by these considerations, in this work we seek to develop a unified framework for sensor fault-tolerant control of sampled-data process systems with measurement delays that offers further insights into both the limitations imposed by sensor faults and measurement delays on the performance and stability of the closed-loop system, and the possible fault accommodation strategies that incorporate both stability and performance considerations. This framework offers a more comprehensive picture of fault-tolerant control through addressing specifically the performance aspects of the system under sensor faults as a function of various process parameters.

2. PRELIMINARIES

2.1 System description

In this work, we consider the following class of linear continuous-time systems with dynamics captured by a state-space representation of the form:

$$\begin{aligned} \dot{x} &= Ax + Bu \\ y &= \Phi x \end{aligned} \tag{1}$$

where $x \in \mathbb{R}^n$ is the vector of system state variables, $A \in \mathbb{R}^{n\times n}$ and $B \in \mathbb{R}^{n\times m}$ are constant state and input matrices, respectively, describing the system dynamics, $u \in \mathbb{R}^m$ is the vector of manipulated inputs, $y \in \mathbb{R}^n$ is the vector of state measurements, $\Phi = \text{diag}\{\phi_i\} \in \mathbb{R}^{n\times n}$ is a diagonal matrix that indicates the fault or health status of the measurement sensors, where ϕ_i represents the fault in the i-th measurement sensor. A value of $\phi_i = 1$ indicates a healthy sensor, while any other value different from 1 is taken to indicate a faulty sensor. In this representation, sensor faults are basically modeled as either diminished or amplified state measurements. When all measurement sensors are healthy, Φ will be the identity matrix.

Referring to the system of Eq.(1), the control problem considered is that of stabilizing the states of the closed-loop system at desired steady-state values in the presence of measurement sensor faults, while minimizing the closed-loop performance degradation resulting from the sensor faults. This objective is to be achieved using discretely-sampled and delayed state measurements, while accounting for the performance of the post-fault closed-loop system in the selection of an appropriate fault accommodation strategy. For the purposes of this study, it is assumed that a satisfactory method for detecting and estimating the size of the sensor faults is available (whether that be a single estimate of the fault or a range of values that the fault is assumed to be contained within), as well as some means of delay estimation such as time stamping of measurements. These assumptions are made in light of the intended emphasis of this work on the analysis and mitigation aspects of the problem.

2.2 Model-based feedback controller design

In a sampled-data system, measurements of the states of the system of Eq.(1) are not continuously available. This necessitates the use of an inter-sample model predictor to estimate the system states between sampling times in order to provide a continuous control action to the process. To this end, we consider the following system model:

$$\dot{\widehat{x}} = \widehat{A}\widehat{x} + \widehat{B}u \tag{2}$$

where $\widehat{x}$ is the vector of the modeled system states; and $\widehat{A}$ and $\widehat{B}$ are the modeled values of the state and input matrices, A and B, respectively. The difference between the plant matrices (A, B) and the model matrices $(\widehat{A}, \widehat{B})$ describes the plant-model mismatch.

The model of Eq.(2) is embedded within the control system and its states are assumed to be continuously available to the feedback controller. The model-based control action can then be computed as follows:

$$u = K\widehat{x} \tag{3}$$

where K is a constant feedback gain matrix chosen to stabilize the origin of the closed-loop model, where this stability condition is determined by the placement the poles of the closed-loop model.

While the values of $\widehat{x}$ are continuously available to the controller, it is important to periodically update $\widehat{x}$ to match the state of the actual system dynamics and correct for any inaccuracies caused by the plant-model mismatch. The implementation of this model state update is complicated when state measurement delays are involved since updating $\widehat{x}$ using a delayed measurement of the state x introduces unneeded errors in the feedback loop. One way to compensate for such errors is to include within the control system a propagation unit that provides an estimate of the current state of the system based on the delayed measurement. A propagation unit of the following form is used to account for measurement delays:

$$\dot{\bar{x}} = \bar{A}\bar{x} + \bar{B}u \tag{4}$$

where $\bar{x}$ is the state of the propagation unit, $\bar{A}$ and $\bar{B}$ are constant matrices describing the dynamics of the propagation model (note these are not necessarily equal to A, B or $\widehat{A}, \widehat{B}$).

If measurements arrive at the controller after a delay τ from the time the measurements were taken and transmitted, the propagation unit will propagate the state measurements from the transmission time to the current time in order to provide a more accurate estimate of the current state of the system which is then used to update the state of the model. A schematic representation of the model and propagation unit update patterns is depicted in Fig.1 for the case when no sensor faults are present. It can be seen in Fig. 1 that the state of the propagation unit is reset to the state of the system at each transmission time, $t_k - \tau$, where τ represents the length of the delay (which for the purposes of this study is assumed to be known and constant). The sampling period is given by $h = (t_{k+1} - \tau) - (t_k - \tau)$, and without loss of generality, it is assumed that $\tau < h$. It should be noted, however, that this assumption is made

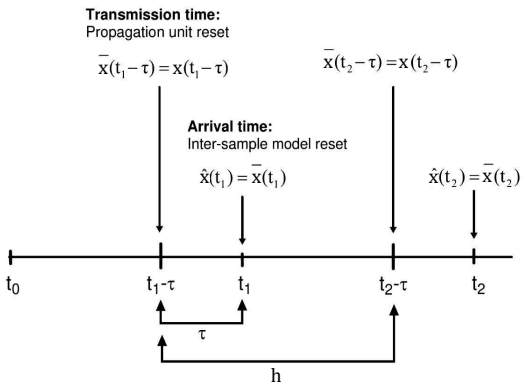

Fig. 1. Model and propagation unit state update patterns using discretely-sampled and delayed measurements.

only to simplify the model and propagation unit update patterns, but can be readily relaxed at the expense of increased complexity in the analysis.

In the presence of sensor faults, the update law for the state of the propagation unit is modified as follows:

$$\bar{x}(t_k-\tau)=y(t_k-\tau)=\Phi x(t_k-\tau) \tag{5}$$

where the Φ is the sensor fault matrix defined earlier in Eq.(1). Note that the presence of sensor faults causes the state of the propagation unit to be updated with a distorted measurement of the system state at each transmission time. Once the state of the propagation unit has been refreshed, it propagates the delayed measurement to the signal arrival time, t_k, and updates the model state of Eq.(2) as follows:

$$\widehat{x}(t_k)=\bar{x}(t_k) \tag{6}$$

It is important to note that for the implementation of this type of delay-handling strategy it is assumed that at each arrival time, t_k, the propagation unit immediately propagates the received measurement over the interval $t\in(t_k-\tau,t_k)$ using the stored control inputs from Eqs.(2)-(3). For this to be possible the delay size τ must be known or estimated.

3. CHARACTERIZATION OF CLOSED-LOOP STABILITY SUBJECT TO SENSOR FAULTS

To elucidate the influences of sensor faults on the stability of the closed-loop system, we proceed in this section to formulate an augmented closed-loop system that captures the collective dynamics of the plant, the controller model and the propagation unit. To this end, we define an augmented state vector $\xi=[x^T\ e_p^T\ e_m^T]^T$, with $e_p=\bar{x}-x$ representing the propagation unit error and $e_m=\widehat{x}-\bar{x}$ representing the model estimation error. With these definitions, the augmented closed-loop system can be represented in the following form:

$$\dot{\xi}=\Lambda\xi \tag{7}$$

where

$$\Lambda=[\,\Lambda_1\ \Lambda_2\ \Lambda_3\,] \tag{8}$$

with

$$\Lambda_1=\begin{bmatrix} A+BK \\ \bar{A}-A+\left(\bar{B}-B\right)K \\ \widehat{A}-\bar{A}+\left(\widehat{B}-\bar{B}\right)K \end{bmatrix}$$

$$\Lambda_2=\begin{bmatrix} BK \\ \bar{A}+\left(\bar{B}-B\right)K \\ \widehat{A}-\bar{A}+\left(\widehat{B}-\bar{B}\right)K \end{bmatrix},\ \Lambda_3=\begin{bmatrix} BK \\ \left(\bar{B}-B\right)K \\ \widehat{A}+\left(\widehat{B}-\bar{B}\right)K \end{bmatrix}$$

It can be shown (using calculations similar to those in Napasindayao and El-Farra (2013)) that the solution to the above augmented closed-loop system takes the following piecewise form:

$$\xi(t)=\begin{cases} e^{\Lambda(t-t_k)}M^k\xi(t_0) \\ \forall t\in[t_k,t_{k+1}-\tau),\forall k\geq 0 \\ \\ e^{\Lambda(t-t_{k+1}+\tau)}I_p e^{\Lambda(h-\tau)}M^k\xi(t_0) \\ \forall t\in[t_{k+1}-\tau,t_{k+1}),\forall k\geq 0 \end{cases} \tag{9}$$

where $h=t_{k+1}-t_k$ is the sampling period, and M is a special matrix that dictates closed-loop stability and is given by:

$$M=I_m e^{\Lambda\tau}I_p e^{\Lambda(h-\tau)} \tag{10}$$

with I_m and I_p defined as follows:

$$I_m=\begin{bmatrix} I & O & O \\ O & I & O \\ O & O & O \end{bmatrix},\ I_p=\begin{bmatrix} I & O & O \\ \Phi-I & O & O \\ I-\Phi & I & I \end{bmatrix} \tag{11}$$

where I represents the identity matrix. The matrices I_m and I_p are referred to as the model and propagation unit update matrices, respectively, since the structures of these matrices are dictated by the model and propagation update logics. Note that the sensor fault parameter Φ manifests itself only in the propagation unit update matrix I_p due to the fact that the state of the propagation unit is updated with a potentially incorrect state measurement as per Eq.(5). The model state, however, is only indirectly influenced by the sensor fault since it is updated using the state of the propagation unit.

Due to the discretely-sampled nature of the state measurements, it can be shown (e.g., see Napasindayao and El-Farra (2013), Garcia et al. (2014)) that closed-loop stability is assured if the maximum eigenvalue magnitude of the stability test matrix M is strictly less than one, i.e.:

$$\lambda_{\max}\Big(M(A,B,\widehat{A},\widehat{B},\bar{A},\bar{B},K,\Phi,h,\tau)\Big)<1 \tag{12}$$

From an operational standpoint, the condition in Eq.(12) can also be leveraged as the basis for the development of stability-based fault accommodation strategies that explicitly account for the effects of all the parameters shown in Eq.(12). Potential measures for mitigating the impact of faults include adjusting any variable parameter in the model as well as the more conventional approach of varying the feedback controller gain, K. For any fault accommodation strategy, the condition in Eq.(12) can be used to explicitly determine a priori if the accommodation measure taken will stabilize the post-fault closed-loop system. For example, for a given plant-model mismatch, sampling period, delay size, and fault size, this condition can be used to determine the range of possible values that an accommodation variable (such as pole location) can assume so as to maintain post-fault closed-loop stability (see Section 5 for a demonstration).

4. CLOSED-LOOP PERFORMANCE CHARACTERIZATION UNDER DELAYS AND SENSOR FAULTS

To analyze the impact of measurement sampling, delays and sensor faults on closed-loop performance, we take the system to be initially at steady-state prior to an impulse perturbation at some time by an external disturbance in a particular input. The performance of the closed-loop system is then characterized in terms of the settling time of some chosen performance output in response to this perturbation. To this end, we consider the following state-space system representation, which now includes the input disturbances:

$$\dot{x}(t) = Ax(t) + Bu(t) + Ew(t) \tag{13}$$

$$z(t) = Jx(t) \tag{14}$$

where $w(t) = \delta(t-t_0) \in \mathbb{R}^{q\times 1}$ is an impulse disturbance at some time t_0 that manifests itself into the plant dynamics through the matrix $E \in \mathbb{R}^{n\times q}$; $z(t)$ is the performance output, and J is the performance output matrix. Based on this representation, it can be shown that the augmented closed-loop system takes the following form:

$$\dot{\xi}(t) = \Lambda\xi + Hw(t) \tag{15}$$

$$z(t) = L\xi(t) \tag{16}$$

where $H = [E^T \ -E^T \ O]^T$ and $L = [J \ O \ O]$, and that the performance output is given by:

$$z(t) = \begin{cases} z_1(t), & \forall t \in [t_k, t_{k+1}-\tau), \forall k \geq 0 \\ \\ z_2(t), & \forall t \in [t_{k+1}-\tau, t_{k+1}), \forall k \geq 0 \end{cases} \tag{17}$$

where

$$\begin{aligned} z_1(t) &= Le^{\Lambda(t-t_k)}M^kH \\ z_2(t) &= Le^{\Lambda(t-t_{k+1}+\tau)}I_pe^{\Lambda(h-\tau)}M^kH \end{aligned} \tag{18}$$

Recall that in general, the H_2-norm is given by:

$$\|G\|_{H_2}^2 = \int_{t_0}^{\infty} z^T(t)z(t)\,dt \tag{19}$$

Substituting the performance output response of Eqs.(17)-(18) into Eq.(19), we obtain the following expression for the extended H_2-norm of the sampled-data closed-loop system:

$$\begin{aligned} \int_{t_0}^{t_\infty} z^T(t)z(t)\,dt = &\sum_{k=0}^{\infty}\left(\int_{t_k}^{t_{k+1}-\tau} z_1^T(t)z_1(t)\,dt\right) \\ &+ \sum_{k=1}^{\infty}\left(\int_{t_k-\tau}^{t_k} z_2^T(t)z_2(t)\,dt\right) \end{aligned} \tag{20}$$

Based on this, it can be shown that the extended H_2-norm can be computed as:

$$\|G\|_{H_2} = trace\left(H^T\left(X_1 + X_2\right)H\right)^{1/2} \tag{21}$$

where X_1 and X_2 are the solutions to the following discrete Lyapunov equations:

$$\begin{aligned} &M^TX_1M - X_1 + W_o\left(0, h-\tau\right) = 0 \\ &M^TX_2M - X_2 + \\ &\left(e^{\Lambda(h-\tau)}\right)^T I_p^T W_o\left(0,\tau\right) I_p e^{\Lambda(h-\tau)} = 0 \end{aligned} \tag{22}$$

with $W_o(0, h-\tau)$ and $W_o(0,\tau)$ defined by:

$$\begin{aligned} W_o\left(0, h-\tau\right) &= \int_0^{h-\tau}\left(e^{\Lambda t}\right)^T L^T L e^{\Lambda t}dt \\ W_o\left(0,\tau\right) &= \int_0^{\tau}\left(e^{\Lambda t}\right)^T L^T L e^{\Lambda t}dt \end{aligned} \tag{23}$$

An examination of the above equations shows that the closed-loop performance metric is characterized in terms of the same process, model, and propagation unit parameters that appear in the closed-loop stability characterization of Eqs.(10) and (12). This characterization of the closed-loop performance can be used in conjunction with the closed-loop stability characterization discussed in Section 3 to explore the interplays between plant-model mismatch, delays, sampling rates, and faults on the closed-loop performance. These interplays are explored in the context of a simulation case study in Section 5. This insight can then be used to develop fault mitigation strategies that not only ensure closed-loop stability but also minimize performance deterioration in the presence of faults.

5. SIMULATION STUDY

To explore the methods developed in Sections 3 and 4, a process composed of a cascade of two non-isothermal continuous-stirred tank reactors with a recycle stream and three parallel irreversible elementary reactions is used as an illustrative example (see Sun and El-Farra (2008) for the process model and model parameters). This process is chosen due to its controllability and thus the ability to place the poles of the closed-loop system at any location. This aids in the illustrative value of this process when assessing fault accommodation measures. The linearized process model of this system can be cast in the form of Eqs.1-4 with the following numerical values for the state and input matrices:

$$A = \begin{bmatrix} 25.30 & 4.97 & 31.75 & 0 \\ -78.03 & -45.94 & 0 & 34.64 \\ 14.70 & 1.42 & -2.84 & 1.42 \\ 0 & 13.47 & -22.45 & -24.88 \end{bmatrix}$$

$$B = \begin{bmatrix} 9.45e^{-6} & 0 & 0 & 0 \\ 0 & 2.82 & 0 & 0 \\ 0 & 0 & 3.47e^{-6} & 0 \\ 0 & 0 & 0 & 5.71 \end{bmatrix} \tag{24}$$

The state and manipulated inputs of the system are defined as $x = [x_1 \ x_2 \ x_3 \ x_4]^T$ and $u = [u_1 \ u_2 \ u_3 \ u_4]^T$, respectively, where x_1 and x_3 are the dimensionless deviations of the temperature in the first and second reactors, respectively; and x_2 and x_4 are the dimensionless deviations of the reactant concentration in the first and second reactors, respectively. Likewise, u_1 and u_3 are the deviation variables for the heat duty and feed-stock concentration to the first reactor; and u_2 and u_4 are the equivalent quantities for

the second reactor. The system is to be operated around the open-loop unstable steady state.

The disturbance input to the system for the simulations was chosen to be the temperature of the feedstock stream into the first reactor. Any plant-model mismatch is reported as a deviation in the modeled estimates of the enthalpy of reaction for all three reactions: $\Delta H_{i,model} = (1+\delta_{\Delta H})\cdot\Delta H_{i,actual}$. This mismatch primarily manifests itself in the deviations in the linearized temperature equations (i.e. the first and third rows of the A matrix), such that $A \neq \widehat{A}$ and $A \neq \bar{A}$. The controller gain K was calculated by placing the poles of the closed loop system model at $\alpha\cdot[-1, -2, -3, -4]$, where α is the primary means of fault accommodation with a baseline value of $\alpha = 1$. Finally, and to simplify the analysis and visualization of the results, the sensor fault matrix was taken to be of the form $\Phi = \phi I$, where ϕ is the fault size which is assumed to be the same for all measured states. It is possible, however, to consider different fault sizes for different measured states.

5.1 Effects of sensor faults and plant-model mismatch

First we will explore the effects that sensor faults and plant-model mismatch have on the stability and performance of the closed-loop system. By leveraging the analysis tools presented in Sections 3 and 4 we can observe how the potential under- and over-estimation of a given process parameter can impact the stability, performance, and tolerable fault range of the system.

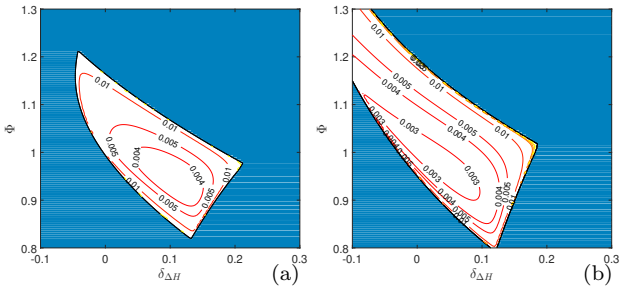

Fig. 2. Contour plot showing the closed-loop stability region (uncolored) and performance contours as a function of the sensor fault ϕ and enthalpy of reaction mismatch $\delta_{\Delta H}$, with a sampling period of $h = 0.05$ hours and delay of $\tau = 0.025$ hours, with (a) the pole placement parameter at its nominal value of $\alpha = 1$ and (b) the pole placement parameter at its largest tested value of $\alpha = 10$.

Fig.2 shows the performance metric obtained in Section 4, where a given contour line inside the white region depicts the settling time (recall that lower values correspond to better performance). The stability region of this process is also shown in this figure: any set of parameter values that fall in the region of solid color correspond to unstable operation.

Nominal process operation, meaning no sensor fault and no plant-model mismatch, corresponds to a value of $\phi = 1$ and $\delta_{\Delta H} = 0$. Note how a relatively small underestimation of the plant-model mismatch (any deviation to the left along the horizontal line at $\phi = 1$) would result in the system being pushed to the unstable region of operation, whereas a much larger perturbation would need to occur in the positive direction to result in instability. This is true for both cases shown in Fig.2. This illustrates the fact that underestimating the heat generated from this exothermic reaction is quite detrimental whereas overestimation of the heat generation actually results in increased performance (to a point). This is believed to be due to the "built-in" aggressiveness in the controller that occurs when the enthalpy of reaction is overestimated.

Comparing Fig.2(a) to Fig.2(b) shows the benefit of the chosen accommodation measure. In the case of nominal operation, Fig.2(a) shows that the region of best performance cannot be obtained with no plant-model mismatch ($\delta_{\Delta H} = 0$). However, when the accommodation variable is adjusted as shown in Fig.2(b), this pushes the region of best performance to overlap with operation of the plant with a perfect model. This also has the added benefit of increasing the range of tolerable faults of the kind $\phi > 1$ that the system can remain operable during. It should also be noted that with the parameters shown in Fig.2, the most effective safeguard against faults that diminish the sensors' output ($\phi < 1$) would be to introduce some positive plant-model mismatch ($\delta_{\Delta H} > 0$).

5.2 Effect of sensor faults and pole placement parameter: active fault accommodation

In this section we will examine the prescribed fault accommodation parameter α, and how it can be adjusted to accommodate for sensor faults. As with the prior section, 5.1, this will be done relative to the sensor faults.

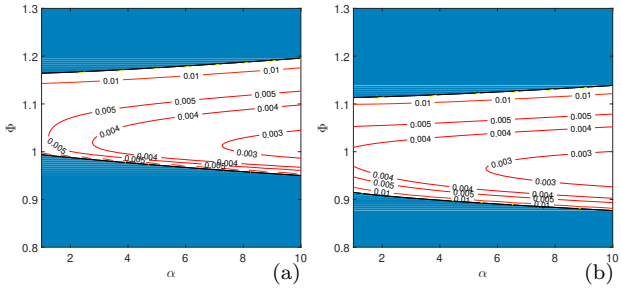

Fig. 3. Contour plot showing the closed-loop stability region (uncolored) and performance contours as a function of the sensor fault ϕ and pole placement parameter α, with a sampling rate of $h = 0.05$ hours and delay of $\tau = 0.025$ hours, with (a) a perfect process model and (b) a plant-model mismatch of $\delta_{\Delta H} = 0.05$.

The trends shown in Fig.3 are consistent with those in Fig.2, where the perfect model does not offer much difference in the magnitude of the tolerable fault ranges across the accommodation variable α when compared to the case with plant-model mismatch. However, the values of the tolerable faults that these can accommodate are quite different. This is consistent with Fig.2, where vertical slices at $\delta_{\Delta H} = 0$ and again at $\delta_{\Delta H} = 0.05$ produce similar fault ranges. Interestingly, due to the stability landscape, the larger the plant-model mismatch the further down the tolerable range is shifted in absolute terms. This has interesting implications to fault-tolerance and operability if these types of trends are known a priori. For example, an operator could intentionally augment some modeled parameters in such a way to provide more "centered" fault-tolerance, or could "hedge" operation in such a way to be more robust to faults in a certain direction.

5.3 Closed-loop simulation results

In this section we consider the dynamic response of the closed-loop system to a disturbance in the case of faults that may be performance-degrading and/or destabilizing. The results in the presence and absence of fault accommodation are compared. The disturbance creates an increase in the temperature of the feed into the first reactor, which due to the kinetics of the three parallel reactions causes the undesirable products to out-compete the desired product leading to a decrease in the desired product concentration (i.e., the performance output decreases).

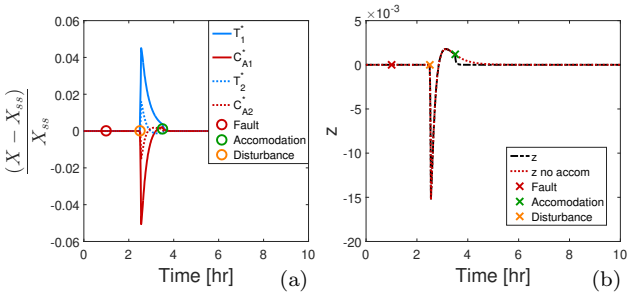

Fig. 4. Illustration of performance-based fault accommodation: Time response of the dimensionless closed-loop states (plot (a)) and performance output (plot (b)) to a performance-degrading fault of $\phi = 1 \rightarrow 1.01 \cdot I$ at $t = 1$ hour, with a disturbance in the inlet temperature at $t = 2.5$ hours, and an accommodation measure of $\alpha = 1 \rightarrow 10$ at $t = 3.5$ hours, with no plant-model mismatch, operating with a sampling period of $h = 0.05$ hours and a delay of 0.025 hours.

Fig.4 illustrates the benefits of performance-based fault accommodation. In the absence of fault accommodation, the system does self-regulate to the prior stable value (as predicted in Fig.3(a)); however, with accommodation it does so in a more timely manner. The inlet temperature disturbance in this instance is solely performance-degrading, as the closed-loop system is able to recover to its pre-fault state values.

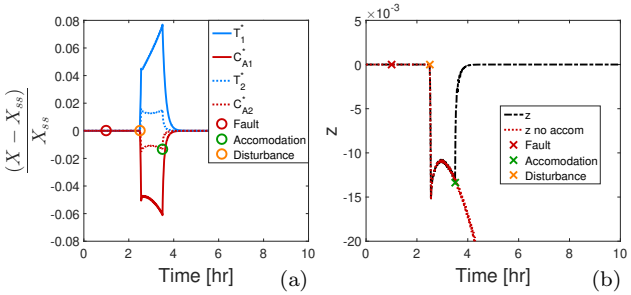

Fig. 5. Illustration of stability-based fault accommodation: Time response of the dimensionless closed-loop states (plot (a)) and the performance output (plot (b)) to a stability-degrading fault of $\phi = 1 \rightarrow 0.99 \cdot I$ at $t = 1$ hour, a disturbance in the inlet temperature at $t = 2.5$ hours, and an accommodation measure of $\alpha = 1 \rightarrow 10$ at $t = 3.5$ hours, with no plant-model mismatch, operating with a sampling period of $h = 0.05$ hours and a delay of 0.025 hours.

Fig.5 illustrates the utility of stability-based fault accommodation. After the system is perturbed post-fault, it is unable to recover until accommodation measures are enacted, which is consistent with the trends shown in Fig.3(a). This disturbance is of the same magnitude as in Fig.4; however, the fault here is a destabilizing one. Although the overall trends are similar to those in Fig.4, in this case the system is unable to recover without the fault being accommodated.

REFERENCES

Allen, J., Chen, S., and El-Farra, N.H. (2019). Model-based strategies for sensor fault accommodation in uncertain dynamic processes with multi-rate sampled measurements. *Chemical Engineering Research and Design*, 142, 204 – 213.

Allen, J.T. and El-Farra, N.H. (2017). A model-based framework for fault estimation and accommodation applied to distributed energy resources. *Renewable Energy*, 100, 35–43.

Blanke, M., Kinnaert, M., Lunze, J., and Staroswiecki, M. (2003). *Diagnosis and Fault-Tolerant Control*. Springer, Berlin-Heidelberg.

Gani, A., Mhaskar, P., and Christofides, P.D. (2008). Handling sensor malfunctions in control of particulate processes. *Chem. Eng. Sci.*, 63, 1217–1229.

Garcia, E., Antsaklis, P.J., and Montestruque, L.A. (2014). *Model-based control of networked systems*. Springer.

Isermann, M. (2005). *Fault-Diagnosis Systems: An Introduction from Fault Detection to Fault Tolerance*. Springer, Berlin.

Mhaskar, P., Liu, J., and Christofides, P.D. (2013). *Fault-Tolerant Process Control: Methods and Applications*. Springer-Verlag, London.

Napasindayao, T. and El-Farra, N.H. (2013). Fault detection and accommodation in particulate processes with sampled and delayed measurements. *Ind. & Eng. Chem. Res.*, 52(35), 12490–12499.

Napasindayao, T. and El-Farra, N.H. (2015). Model-based fault-tolerant control of uncertain particulate processes: Integrating fault detection, estimation and accommodation. In *Proceedings of 9th IFAC Symposium on Advanced Control of Chemical Processes*, 872–877. Whistler, Canada.

Peng, D. and El-Farra, N.H. (2015). Integrated identification and accommodation of sensor faults in networked distributed processes with communication delays. In *Proceedings of American Control Conference*, 1284–1289. Chicago, IL.

Sun, Y. and El-Farra, N.H. (2008). Quasi-decentralized model-based networked control of process systems. *Comp. & Chem. Eng.*, 32, 2016–2029.

Sun, Y. and El-Farra, N.H. (2011). Model-based fault detection and fault-tolerant control of process systems with sampled and delayed measurements. In *Proceedings of 18th IFAC World Congress*, 2749–2754. Milan, Italy.

Yao, Z. and El-Farra, N.H. (2014). Performance-based sensor reconfiguration for fault-tolerant control of uncertain spatially distributed processes. In *Proceedings of 19th IFAC World Congress*, 5193–5198. Cape Town, South Africa.